ASTROBIOLOGY

ALMA detection and astrobiological potential of vinyl cyanide on Titan

Maureen Y. Palmer,[1,2,3]* Martin A. Cordiner,[1,3] Conor A. Nixon,[1] Steven B. Charnley,[1] Nicholas A. Teanby,[4] Zbigniew Kisiel,[5] Patrick G. J. Irwin,[6] Michael J. Mumma[1]

Recent simulations have indicated that vinyl cyanide is the best candidate molecule for the formation of cell membranes/vesicle structures in Titan's hydrocarbon-rich lakes and seas. Although the existence of vinyl cyanide (C_2H_3CN) on Titan was previously inferred using Cassini mass spectrometry, a definitive detection has been lacking until now. We report the first spectroscopic detection of vinyl cyanide in Titan's atmosphere, obtained using archival data from the Atacama Large Millimeter/submillimeter Array (ALMA), collected from February to May 2014. We detect the three strongest rotational lines of C_2H_3CN in the frequency range of 230 to 232 GHz, each with >4σ confidence. Radiative transfer modeling suggests that most of the C_2H_3CN emission originates at altitudes of ≳200 km, in agreement with recent photochemical models. The vertical column densities implied by our best-fitting models lie in the range of 3.7×10^{13} to 1.4×10^{14} cm^{-2}. The corresponding production rate of vinyl cyanide and its saturation mole fraction imply the availability of sufficient dissolved material to form ~10^7 cell membranes/cm^3 in Titan's sea Ligeia Mare.

INTRODUCTION

Titan is one of the most interesting bodies in our Solar System, with complex organic chemistry, a thick nitrogen-based atmosphere, and bodies of liquid on the surface. Titan's atmospheric chemistry and atmosphere-surface interactions are not well understood, and improved knowledge of these processes not only helps us understand Titan's particular chemical history but provides insights into the processes that shape our own planet's climate and atmospheric composition. Titan differs from Earth in several important ways, with an average surface temperature of only 94 K. As a result, all surface water is frozen, and the lakes and seas are instead thought to be mostly composed of methane and ethane (*1*). This presents an issue for the development of life, because lipid membranes, which are common to Earthly organisms, could not exist in cryogenic methane. Cell membrane–like compartments are crucial for the development of life from a sea of prebiotic reactants. These membranes enclose a small volume of solution, where reactants can be concentrated and (pre)biotic reactions can occur with greater frequency than they would in the dilute environment of an entire lake or sea. They also define individual cells as separate from each other, creating the potential for competition and natural selection. Recent simulations have investigated some nitrile species for their potential to form flexible membranes in Titan-like conditions. These simulations suggest that vinyl cyanide (C_2H_3CN; also known as acrylonitrile or propenenitrile) would be the best candidate species for the formation of these hypothesized cell-like membranes, known as "azotosomes" (*2*).

Previous studies have suggested the likely existence of vinyl cyanide on Titan, but it has not yet been conclusively detected. Whereas laboratory simulations of Titan's atmosphere produce significant amounts of vinyl cyanide (*3*), previous spectroscopic searches have been inconclusive: Infrared Space Observatory (ISO) spectra showed no evidence for C_2H_3CN emission (*4*). A stratospheric abundance upper limit of 2×10^{-9} was obtained from observations with the Institut de Radioastronomie Millimétrique (IRAM) 30-m (radio) telescope (*5*, *6*). Vinyl cyanide has been suggested as a possible constituent of Titan's surface ices, but the 5.01-μm Cassini VIMS (Visual and Infrared Mapping Spectrometer) spectrum does not provide a good match with laboratory C_2H_3CN ice data (*7*).

The strongest previous evidence for C_2H_3CN on Titan was the detection of $C_2H_3CNH^+$ by the Cassini Ion and Neutral Mass Spectrometer (INMS) (*8*). This nitrile ion was theorized to form primarily by proton transfer to neutral C_2H_3CN. The presence of the neutral molecule was also inferred using the INMS in closed-source neutral (CSN) mode (*9*, *10*). By fitting the INMS CSN signal using cracking patterns of multiple species, a C_2H_3CN abundance of 3.5×10^{-7} at 1050 km was determined on the basis of the observed fragments, but the C_2H_3CN molecule itself was not clearly seen (*10*). A millimeter-wave spectroscopic detection would provide the first definitive proof for the presence of C_2H_3CN and would help validate the conclusions of the INMS studies. Gas-phase synthesis of C_2H_3CN is not well understood. Measurements of the vinyl cyanide atmospheric distribution are needed to constrain models for the formation of nitriles and other compounds in Titan's atmosphere, which will lead to improvements in our understanding of its complex photochemistry and provide new insights into the chemistry of primitive terrestrial (exo)planetary atmospheres.

Here, we used data from the Atacama Large Millimeter/submillimeter Array (ALMA) Science Archive (https://almascience.nrao.edu/alma-data/archive) to search for rotational emission lines from C_2H_3CN in Titan's atmosphere. Interferometric observations of Titan are made routinely using ALMA for the purpose of flux calibration. The present study incorporates 11 flux calibration measurement sets, obtained by ALMA during the period of 22 February 2014 to 27 May 2014. To search for new molecules, our strategy involved combining multiple measurement sets spanning the frequency range of interest to reduce the noise level and provide unprecedented sensitivity for molecular detections at millimeter wavelengths. We report the detection of three rotational lines of C_2H_3CN. The line profiles are found to be

[1]NASA Goddard Space Flight Center, 8800 Greenbelt Road, Greenbelt, MD 20771, USA. [2]Department of Chemistry, St. Olaf College, 1520 St. Olaf Avenue, Northfield, MN 55057, USA. [3]Department of Physics, Catholic University of America, Washington, DC 20064, USA. [4]School of Earth Sciences, University of Bristol, Wills Memorial Building, Queens Road, Bristol BS8 1RJ, UK. [5]Institute of Physics, Polish Academy of Sciences, Al. Lotników 32/46, 02-668 Warszawa, Poland. [6]Atmospheric, Oceanic and Planetary Physics, Clarendon Laboratory, University of Oxford, Parks Road, Oxford OX1 3PU, UK.
*Corresponding author. Email: maureen.y.palmer@nasa.gov

consistent with production predominantly at high altitudes, and we calculate that vinyl cyanide will likely reach saturation in Titan's lakes.

RESULTS

The observed spectra are shown in Fig. 1. All three targeted C_2H_3CN lines were detected at precisely the correct frequency [obtained from laboratory measurements (*11*)] and with greater than 4σ confidence; their integrated fluxes and 1σ errors are given in Table 1. The detection of all expected lines of C_2H_3CN in this wavelength region (given the spectroscopic noise level, calculated from continuum regions near the lines of interest) adds confidence to our spectroscopic assignments. Other C_2H_3CN lines in the spectral range covered by our data are expected to be weaker by at least a factor of 20. An integrated map of the detected C_2H_3CN flux (fig. S1) shows that the signal is from a well-confined region, centered on Titan's disc. There is tentative evidence (at the 2σ level) for enhanced C_2H_3CN emission from Titan's southern (winter) hemisphere, but the signal-to-noise ratio and angular resolution are insufficient for a proper analysis of the latitudinal distribution of this species.

We used radiative transfer modeling to constrain the abundance and altitude of vinyl cyanide in the atmosphere (see Materials and Methods for details). We tested four simple "step" models. In these models, we assumed a constant C_2H_3CN abundance above a given cutoff altitude (z_r), with zero below. This enables us to constrain the lower bound of the flux contribution and to provide an estimate of the total C_2H_3CN column density. We also tested a fractional scale height (FSH) model, with a smoothly varying altitude dependence; the abundance at 300 km and the FSH were both allowed to vary until the best fit to the observations was obtained. The best-fitting model abundance profiles are shown in Fig. 2, and the corresponding spectra are overlaid on the observed spectra in Fig. 1. The best fit is for z_r = 300 km, whereas a poor fit is obtained for z_r < 200 km, which implies that most of the observed C_2H_3CN is at stratospheric/mesospheric altitudes of >200 km. The lack of detectable pressure broadening in our observed C_2H_3CN line profiles allows us to reject the lowest-altitude (z_r = 100 km) model. The C_2H_3CN vertical column densities implied by our best-fitting models lie in the range of 3.7×10^{13} to 1.4×10^{14} cm^{-2} (see Table 2 for all model parameters and results). The true C_2H_3CN vertical profile is likely to be more complex than the simplified profiles

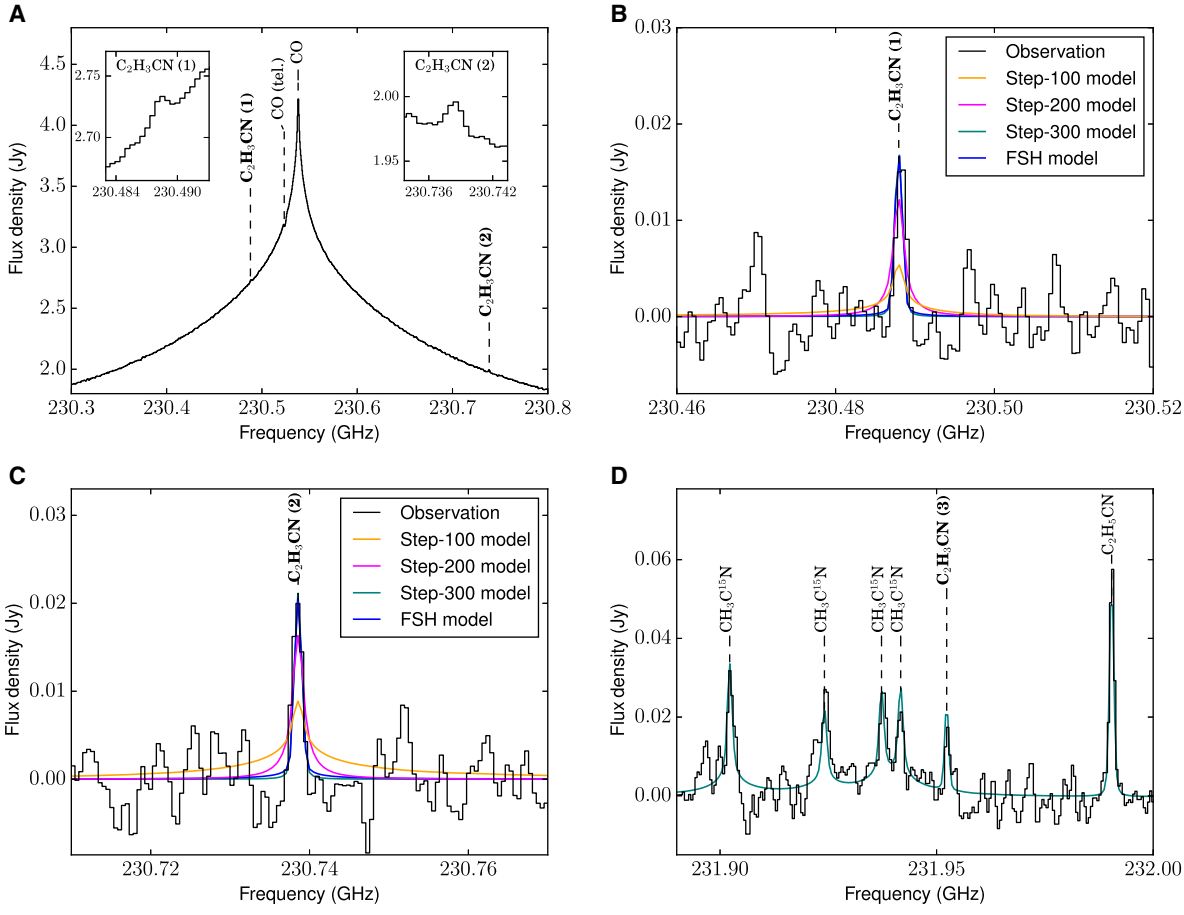

Fig. 1. ALMA spectra showing three detected transitions of C_2H_3CN. (**A**) Observed ALMA spectrum of Titan in the vicinity of the CO *J* = 2–1 line. Detected molecular transitions are labeled; insets show zoomed C_2H_3CN lines in this region. An absorption feature due to telluric CO is also present, redshifted from Titan's CO rest frequency. Flux densities are shown in units of Janskys (Jy). (**B** and **C**) Zoomed, baseline-subtracted spectra of the regions surrounding the two transitions of C_2H_3CN detected in (A). Best-fitting NEMESIS models using various vertical abundance profiles are overlaid. (**D**) Spectral region surrounding the third detected C_2H_3CN transition, with a best-fitting 300-km step model overlaid (the other model curves are omitted from this panel for clarity). Detected lines of C_2H_5CN and $CH_3C^{15}N$ are labeled. Our detection of $CH_3C^{15}N$ may be the first definitive extraterrestrial detection of this acetonitrile isotopolog.

Table 1. Detected C_2H_3CN transitions and line fluxes. Molecular line frequencies are from Kisiel *et al.* (*11*). Line fluxes and 1σ errors were obtained from the continuum-subtracted ALMA spectra.

Line	Frequency (MHz)	Transition	E_u (K)	Flux (Jy·kHz)
C_2H_3CN (1)	230488	$24_{1,23}$–$23_{1,22}$	141	24 ± 4
C_2H_3CN (2)	230739	$25_{0,25}$–$24_{0,24}$	146	28 ± 4
C_2H_3CN (3)	231952	$24_{2,22}$–$23_{2,21}$	147	25 ± 6

adopted here and may be elucidated by future observations that measure the spectral line shapes at higher sensitivity.

We also compare the observed ALMA spectra with theoretical line shapes predicted by atmospheric chemical models. The photochemical models of Wilson and Atreya (*12*), Lavvas *et al.* (*13*), Krasnopolsky (*14*), and Willacy *et al.* (*15*) suggest C_2H_3CN formation primarily by the reaction of CN with C_2H_4 in Titan's upper atmosphere and through the reaction of HCN with C_2H_3 in the lower stratosphere. On the other hand, the recent chemical models of Loison *et al.* (*16*) and Dobrijevic *et al.* (*17*) determined a low efficiency for the HCN + C_2H_3 reaction and found that the C_2H_3CN abundance increases steeply with altitude above 600 km. Abundance profiles from the chemical models of Dobrijevic *et al.* (*17*) and Krasnopolsky (*14*) are shown in Fig. 2. Using our radiative transfer model, the Krasnopolsky profile produces strong pressure-broadened line wings that do not match with the observations (resulting in a reduced χ^2 value of 1.32 and probability $P < 0.0001$). This provides evidence for a low efficiency for the reaction HCN + $C_2H_3 \rightarrow C_2H_3CN$ + H (responsible for the model abundance peak around 100 km) and suggests that the (high-altitude) CN + C_2H_4 reaction is more important for total C_2H_3CN production. The model of Dobrijevic *et al.* is consistent with our observed line shapes ($\chi^2 = 1.04$; $P = 0.31$), provided that their calculated abundance profile is scaled up by a constant factor of 4.7. The need for this enhanced C_2H_3CN production in the upper atmosphere may imply that the rate of the reaction CN + $C_2H_3 \rightarrow C_2H_3CN$ + H was underestimated in their model. It might also imply that there is a polar enhancement for C_2H_3CN, which would result in our disc-averaged measurement being higher than their equatorial model. Future higher-sensitivity observations will be needed to investigate this.

Our C_2H_3CN detection is also helpful as a test and validation of the Cassini INMS studies. Our FSH model is in close agreement with the C_2H_3CN abundance derived at 1100 km (*8*). The abundances found at 1050 km (*9*, *10*) are somewhat lower than our modeled abundances but still within our margin of error. Our 100-km step model is similar to the upper limit previously obtained using IRAM (*5*, *6*).

The lines from other nitriles in our spectra allow our understanding of the chemistry of these related compounds to be explored. Our best-fitting C_2H_5CN abundance is 7.2 ± 0.29 ppb, and the corresponding C_2H_5CN/C_2H_3CN abundance ratio is 2.5 ± 0.3 (using a 300-km step model for both species). This matches the previously observed pattern for Titan's hydrocarbons, in which alkanes are more abundant than alkenes (*18*), and is consistent with a greater chemical stability for alkanes due to shielding by CH_4 and the susceptibility of alkenes to addition reactions at the double bond (*16*).

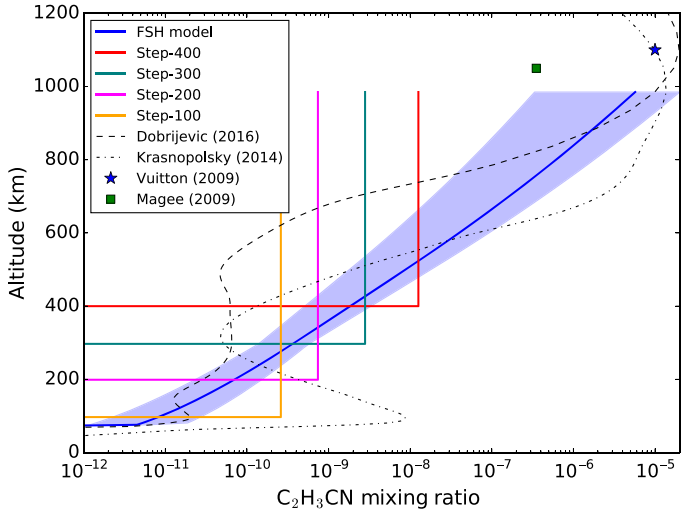

Fig. 2. Best-fitting C_2H_3CN vertical abundance profiles derived using NEMESIS (solid lines). The 300-km step and FSH models provide the best fit to our observations (see Table 2). Profiles from photochemical models are shown for comparison [from Krasnopolsky (*14*) and Dobrijevic *et al.* (*17*); dotted lines], along with the previously inferred ionospheric abundances from Cassini mass spectrometry [from Vuitton *et al.* (*8*) and Magee *et al.* (*10*)]. Light blue region denotes 1σ error limits on the FSH model.

DISCUSSION

Confirmation of the presence of vinyl cyanide on Titan is especially interesting with respect to the possibility of cell membrane–like azotosomes (*2*). Cell membranes are a crucial component of any living organism, and simulations indicate that, at the temperature of Titan's methane lakes, vinyl cyanide (as opposed to other small organic molecules) would form the most stable membranes (*2*). A rain of haze particles continually carries organics, which form in the upper atmosphere, down to the surface, where they can participate in prebiotic or biotic reactions (*19*). Reactions of hydrocarbons with hydrogen, both readily available on Titan, release energy, which could provide support for methanogenic life (*20*). The sedimentation time of atmospheric organics depends on the particle size and convective activity in the troposphere (*21*). This coupling of Titan's atmosphere and surface completes the picture regarding the astrobiological importance of our detection of vinyl cyanide in Titan's middle/upper atmosphere.

With this in mind, it is interesting to estimate how much vinyl cyanide could be in Titan's seas, for example, in Ligeia Mare (Titan's second largest liquid body) located near the northern pole. This can be done using the ratio of net C_2H_3CN production to net ethane production rates from the model of Dobrijevic *et al.* (*17*) (5×10^{-3}), multiplied by 4.7 to account for the scaling factor applied to their modeled abundance to match our data. We assume that C_2H_3CN is predominantly in the condensed phase at the tropopause so that the relationship between production rate and absolute saturation rate is linear. Adopting a range for the proportion of ethane in Ligeia Mare (8 to 33%) (*22*, *23*), the total volume of liquid in Ligeia Mare (14,000 km^3) (*24*) implies a mass of ~10^{13} to 10^{15} kg of C_2H_3CN in this sea. Dubouloz *et al.* (*25*) determined a saturation mole fraction of 2.2×10^{-5} for C_2H_3CN in Titan's oceans, which provides an upper limit for the amount of C_2H_3CN molecules in solution. Our calculated C_2H_3CN abundance implies that vinyl cyanide would reach saturation in Titan's seas (with the excess forming a solid precipitate).

Table 2. Best-fitting C_2H_3CN model abundances.

Model	Abundance (parts per billion)	z_r (km)	N (cm^{-2})	χ^2	P
Step (100 km)	0.26 ± 0.04	100	4.9×10^{14}	1.25	0.001
Step (200 km)	0.74 ± 0.07	200	1.0×10^{14}	1.07	0.19
Step (300 km)	2.83 ± 0.24	300	5.3×10^{13}	1.01	0.44
Step (400 km)	12.6 ± 1.1	400	3.7×10^{13}	1.02	0.40
FSH model	0.36 ± 0.22	297	1.4×10^{14}	1.02	0.37

For an azotosome size of 10 μm, the surface area taken by each molecule of C_2H_3CN (11.3 $Å^2$) and the saturation mole fraction of vinyl cyanide suggest that 4×10^{26} vesicles could be formed, which corresponds to 3×10^7 azotosomes/cm^3 in Ligeia Mare. The actual ethane fraction may be lower than assumed by Dubouloz *et al.*, which is predicted to reduce the amount of dissolved C_2H_3CN by a small amount. On the other hand, the increased stability of azotosome structures compared with free C_2H_3CN suggests that they could incorporate more vinyl cyanide than could completely dissolve. Even a significantly reduced abundance of vinyl cyanide in the liquid or a much smaller fraction of molecules converted into azotosomes could still have great astrobiological significance; for comparison, coastal ocean waters on Earth have ~10^6 bacteria/cm^3 (*26*).

New laboratory studies of gas-phase reactions that form C_2H_3CN are needed to better understand the origin of this molecule on Titan and in other extraterrestrial environments. Experimental studies of membrane formation in cryogenic methane would help assess the viability of azotosome formation. Infrared observations of Titan's aerosol particles could identify the presence of condensed vinyl cyanide and provide insight into its transport to the surface (*27*). ALMA observations with improved signal-to-noise ratio will permit the first detailed maps of the spatial distribution of C_2H_3CN, including abundance measurements over the northern seas and lakes, and will help to further constrain models for Titan's complex organic chemistry and provide new insights into the possibility of incorporation of atmospheric photochemical products into potentially prebiotic structures in Titan's hydrocarbon seas.

MATERIALS AND METHODS

Observations

This study makes use of ALMA data sets #2012.1.00198.S, #2012.1.00261.S, #2012.1.00336.S, #2012.1.00437.S, and #2012.1.00635.S, collected from February to May 2014. Observational parameters for these data sets can be found in table S1. These data were chosen due to their coverage of some of the strongest lines of C_2H_3CN in the ALMA waveband [assuming an excitation temperature of 150 to 170 K (*28*), appropriate for Titan's middle/upper atmosphere, where nitriles have been previously found to be most abundant], including the $24_{1,23}$ to $23_{1,22}$, $25_{0,25}$ to $25_{0,24}$, and $24_{2,22}$ to $23_{2,21}$ transitions, with upper-state energies given in Table 1. The spatial resolution (θ_{min}) of the selected observations was well matched to the size of Titan's (≈0.8″) disc. The high spectral resolution (488 to 976 kHz) makes these data well suited to the detection of weak lines from Titan's upper stratosphere and mesosphere [atmospheric regions less well explored by Cassini (*29*)], where the line shapes are dominated by thermal (Doppler) broadening and are therefore narrow [see also the study of Cordiner *et al.* (*30*)]. Weather conditions were excellent for these observations, with good interferometric phase stability and 0.6 to 2.1 mm of precipitable water vapor (PWV) at zenith.

The data obtained from the ALMA Science Archive were calibrated using standard scripts provided by the Joint ALMA Observatory. This included routine flagging, bandpass calibration, complex gain calibration, and flux calibration. The scripts were modified such that Titan's known emission lines (in particular, the strong CO J = 2–1 line at 231.5 GHz) were not flagged.

Data processing was carried out using CASA (Common Astronomy Software Applications version 4.3.1) (*31*). Using the fixplanets task, Titan's ephemerides (including spatial position and Doppler motion) as a function of time were used to correct each data set to a common coordinate system. The measurement sets were Doppler-shifted to Titan's rest frame and resampled to a common frequency grid using cvel, with 488 kHz per channel (resulting in a Hanning-smoothed spectral resolution of 976 kHz or 1.3 km s^{-1}). Finally, the data were concatenated into combined measurement sets spanning two frequency ranges (230.2 to 230.9 GHz, covering C_2H_3CN lines 1 and 2, and 231.7 to 232.4 GHz, covering line 3), with weightings derived from the root mean square (RMS) noise levels of the respective visibility amplitudes.

To produce spectral/spatial (three-dimensional) data cubes, the interferometric data were imaged using the clean task. The point spread function was deconvolved for each spectral channel using the Högbom algorithm, with natural visibility weighting and a threshold of 5 mJy (approximately twice the RMS noise level). The image pixel sizes were set to 0.1″ × 0.1″, and deconvolution was performed within a 1.7″ × 1.7″ square box centered on Titan. By combining all the observations, the RMS noise per channel was reduced to 2.3 to 2.4 mJy per beam.

Titan's continuum emission was not spatially well resolved in our data, with a shape dominated by the elliptical ALMA restoring beam. Spectra were obtained by integrating the reduced data cubes within an elliptical contour (2.4″ × 1.4″) containing 90% of Titan's continuum flux. This region includes most of the spectral line emission while excluding background noise (off Titan's limb) as much as possible, thus improving the signal-to-noise ratio for the weak spectral features we seek.

Spectral peaks were assigned using the Splatalogue database for astronomical spectroscopy (www.cv.nrao.edu/php/splat/). The C_2H_3CN line frequencies are from Kisiel *et al.* (*11*) and provide an identical match with the observed transitions for this molecule. Unambiguous line assignment is facilitated by the high spectral resolution of our ALMA data; contamination from other species was ruled out by comparison of our spectra with line catalogs, including those species known or predicted to be present in Titan's atmosphere (*14*, *32*).

A map of the C_2H_3CN emission (fig. S1) was produced by subtracting a first- or second-order fit to the continuum adjacent to each of the three detected lines. The remaining line fluxes were then integrated along the spectral axis to produce a (2D) spatial image.

Models

The spatially integrated emission lines were modeled using the line-by-line module of the NEMESIS atmospheric radiative transfer code (*33*). The atmospheric model temperature profile was derived from a combination of Cassini CIRS (Composite Infrared Spectrometer) and HASI (Huygens Atmospheric Structure Instrument) measurements, refined

for the April 2014 epoch using ALMA CO data (*34*). The abundances of nitrogen and methane isotopologs and aerosols were the same as used previously by Teanby *et al.* (*35*). Spectral line parameters and partition functions were taken from the Cologne Database for Molecular Spectroscopy catalog (*36*). For C_2H_3CN, the partition function includes low-lying vibrational modes (with energies up to about 1000 K); contributions from additional modes are calculated to be <0.6% at 200 K. For C_2H_5CN, vibrational modes were not included, but their contribution at 200 K is expected to be <2%. The Lorentzian broadening half-width at 300 K was assumed to be 0.075 cm^{-1} bar^{-1}, with a temperature dependence exponent of 0.50, which is the same as used previously for HC_3N (*37*) and C_2H_5CN (*30*).

The flux scale of our ALMA data was initially calibrated using the standard CASA Butler-JPL-Horizons 2012 flux model for Titan. Because of uncertainties in the vertical temperature profile and CO abundance of that model, we rescaled our spectra to match the more recent (April 2014) model of Serigano *et al.* (*33*). During subsequent spectral line modeling, the sloping pseudocontinuum (consisting of contributions from N_2 and CH_4 collisionally induced absorption as well as CO line emission) was subtracted from our data to provide a clearer view of the weak C_2H_3CN features.

The model fluxes were calculated by integrating (with a linear interpolation scheme) over the radiances obtained across 35 synthetic impact parameters, distributed from the center of Titan's disc to the edge of the model atmosphere at an altitude of 1000 km, and each ray was weighted by a kernel defined by the shape of the (elliptical) flux extraction aperture, convolved with the instrumental point spread function. For these "disc-averaged" models, we assume that Titan's temperature/abundance/aerosol profiles do not vary with latitude and longitude. Initially, least-squares fits to the observed spectra were performed using C_2H_3CN abundance profiles with constant mixing ratio above a specified reference altitude z_r and zero abundance below. In these step models, z_r values in the range of 100 to 400 km were tried. A smoothly varying fractional scale height (FSH) model (*38*) was also tested, for which the abundance at reference altitude (z_r = 300 km) and the FSH value were allowed to vary. In this model, C_2H_3CN was assumed to precipitate out in the troposphere following the saturation law given by Loison *et al.* (*16*). The retrieved parameter values and their associated (1σ) errors are given in Table 2.

Previous studies have observed enhanced nitrile abundances over Titan's winter pole (*39*). At the time of our observations, Titan's north pole was tilted toward Earth by 22°, so the southern (winter) pole was obscured from view behind Titan's disc. Our disc-averaged radiative transfer models could therefore underestimate the C_2H_3CN abundance due to missed polar flux. More detailed measurements of the C_2H_3CN distribution to confirm a polar enhancement will require dedicated ALMA observations at higher sensitivity and angular resolution. If the abundance is sufficiently enhanced at the pole(s), measurements of C_2H_3CN may also be possible in the infrared (for example, using archival Cassini CIRS data) through observations of rovibrational emission. (There is a need for laboratory vibrational spectroscopy of this species because no infrared line list yet exists.)

Our final models (Table 2) are based on simultaneous fits to the two C_2H_3CN lines in spectral region 1 (on either side of the CO line peak; Fig. 1, A to C). The third line was excluded because of the presence of overlapping line wings from the adjacent (pressure broadened) lines of $CH_3C^{15}N$ (Fig. 1D), which render this line unreliable as a probe of the C_2H_3CN vertical abundance profile. Nevertheless, our best-fitting radiative transfer models provide a good fit to the shape and strength of this line, so its identification is secure. We also detected two lines of the related ethyl cyanide molecule (C_2H_5CN), which were modeled using a 300-km step profile [after Cordiner *et al.* (*30*)]. For $CH_3C^{15}N$, we used a scaled version of the CH_3CN vertical profile derived by Marten *et al.* (*6*), where the scaling factor represents the $^{15}N/^{14}N$ ratio of CH_3CN. Assuming negligible change in the disc-averaged CH_3CN vertical profile since the measurements of Marten *et al.*, our best-fitting model for $CH_3C^{15}N$ implies a mean $CH_3CN/CH_3C^{15}N$ ratio of 89 ± 5. The quality of all our model fits was monitored using the reduced χ^2 statistic and associated *P* value, which is the probability that, if the models really matched our observed spectra, we would see such a deviation between them due to chance alone. The resulting fit parameters are given in Table 2, along with the vertical column densities corresponding to each model.

SUPPLEMENTARY MATERIALS

Supplementary material for this article is available at http://advances.sciencemag.org/cgi/content/full/3/7/e1700022/DC1

fig. S1. Integrated flux contour map for C_2H_3CN, summed over the three detected transitions.
table S1. Observational parameters.

REFERENCES AND NOTES

1. K. L. Mitchell, M. B. Barmatz, C. S. Jamieson, R. D. Lorenz, J. I. Lunine, Laboratory measurements of cryogenic liquid alkane microwave absorptivity and implications for the composition of Ligeia Mare, Titan. *Geophys. Res. Lett.* **42**, 1340–1345 (2015).
2. J. Stevenson, J. Lunine, P. Clancy, Membrane alternatives in worlds without oxygen: Creation of an azotosome. *Sci. Adv.* **1**, e1400067 (2015).
3. D. W. Clarke, J. C. Joseph, J. P. Ferris, The design and use of a photochemical flow reactor: A laboratory study of the atmospheric chemistry of cyanoacetylene on Titan. *Icarus* **147**, 282–291 (2000).
4. A. Coustenis, A. Salama, B. Schulz, S. Ott, E. Lellouch, T. Encrenaz, D. Gautier, H. Feuchtgruber, Titan's atmosphere from ISO mid-infrared spectroscopy. *Icarus* **161**, 383–403 (2003).
5. T. Hidayat, Observations heterodynes millimetriques et submillimetriques de Titan: Etude de la composition chimique de son atmosphere, thesis, Universite de Paris-Meudon (1997).
6. A. Marten, T. Hidayat, Y. Biraud, R. Moreno, New millimeter heterodyne observations of Titan: Vertical distributions of nitriles HCN, HC_3N, CH_3CN, and the isotopic ratio $^{15}N/^{14}N$ in its atmosphere. *Icarus* **158**, 532–544 (2002).
7. R. N. Clark, J. M. Curchin, J. W. Barnes, R. Jaumann, L. Soderblom, D. P. Cruikshank, R. H. Brown, S. Rodriguez, J. Lunine, K. Stephan, T. M. Hoefen, S. Le Mouélic, C. Sotin, K. H. Baines, B. J. Buratti, P. D. Nicholson, Detection and mapping of hydrocarbon deposits on Titan. *J. Geophys. Res. Planets* **115**, E10005 (2010).
8. V. Vuitton, R. V. Yelle, M. J. McEwan, Ion chemistry and N-containing molecules in Titan's upper atmosphere. *Icarus* **191**, 722–742 (2007).
9. J. Cui, R. V. Yelle, V. Vuitton, J. H. Waite Jr., W. T. Kasprzak, D. A. Gell, H. B. Niemann, I. C. F. Müller-Wodarg, N. Borggren, G. G. Fletcher, E. L. Patrick, E. Raaen, B. A. Magee, Analysis of Titan's neutral upper atmosphere from Cassini Ion Neutral Mass Spectrometer measurements. *Icarus* **200**, 581–615 (2009).
10. B. A. Magee, J. H. Waite, K. E. Mandt, J. Westlake, J. Bell, D. A. Gell, INMS-derived composition of Titan's upper atmosphere: Analysis methods and model comparison. *Planet. Space Sci.* **57**, 1895–1916 (2009).
11. Z. Kisiel, L. Pszczółkowski, B. J. Drouin, C. S. Brauer, S. Yu, J. C. Pearson, The rotational spectrum of acrylonitrile up to 1.67 THz. *J. Mol. Spectrosc.* **258**, 26–34 (2009).
12. E. H. Wilson, S. K. Atreya, Current state of modeling the photochemistry of Titan's mutually dependent atmosphere and ionosphere. *J. Geophys. Res. Planets* **109**, E06002 (2004).
13. P. P. Lavvas, A. Coustenis, I. M. Vardavas, Coupling photochemistry with haze formation in Titan's atmosphere, Part I: Model description. *Planet. Space Sci.* **56**, 27–66 (2008).
14. V. A. Krasnopolsky, Chemical composition of Titan's atmosphere and ionosphere: Observations and the photochemical model. *Icarus* **236**, 83–91 (2014).
15. K. Willacy, M. Allen, Y. Yung, A new astrobiological model of the atmosphere of Titan. *Astrophys. J.* **829**, 79 (2016).
16. J. C. Loison, E. Hébrard, M. Dobrijevic, K. M. Hickson, F. Caralp, V. Hue, G. Gronoff, O. Venot, Y. Bénilan, The neutral photochemistry of nitriles, amines and imines in the atmosphere of Titan. *Icarus* **247**, 218–247 (2015).

17. M. Dobrijevic, J. C. Loison, K. M. Hickson, G. Gronoff, 1D-coupled photochemical model of neutrals, cations and anions in the atmosphere of Titan. *Icarus* **268**, 313–339 (2016).
18. C. A. Nixon, D. E. Jennings, B. Bézard, S. Vinatier, N. A. Teanby, K. Sung, T. M. Ansty, P. G. J. Irwin, N. Gorius, V. Cottini, A. Coustenis, F. M. Flasar, Detection of propene in Titan's stratosphere. *Astrophys. J. Lett.* **776**, L14 (2013).
19. F. Raulin, T. Owen, Organic chemistry and exobiology on Titan. *Space Sci. Rev.* **104**, 377–394 (2002).
20. C. P. McKay, H. D. Smith, Possibilities for methanogenic life in liquid methane on the surface of Titan. *Icarus* **178**, 274–276 (2005).
21. R. D. Lorenz, The life, death and afterlife of a raindrop on Titan. *Planet. Space Sci.* **31**, 647–655 (1993).
22. S. P. Tan, J. S. Kargel, G. M. Marion, Titan's atmosphere and surface liquid: New calculation using Statistical Associating Fluid Theory. *Icarus* **222**, 53–72 (2013).
23. S. P. Tan, J. S. Kargel, D. E. Jennings, M. Mastrogiuseppe, H. Adidharma, G. M. Marion, Titan's liquids: Exotic behavior and its implications on global fluid circulation. *Icarus* **250**, 64–75 (2015).
24. A. G. Hayes, The lakes and seas of Titan. *Annu. Rev. Earth Planet. Sci.* **44**, 57–83 (2016).
25. N. Dubouloz, F. Raulin, E. Lellouch, D. Gautier, Titan's hypothesized ocean properties: The influence of surface temperature and atmospheric composition uncertainties. *Icarus* **82**, 81–96 (1989).
26. K. E. Wommack, R. R. Colwell, Virioplankton: Viruses in aquatic ecosystems. *Microbiol. Mol. Biol. Rev.* **64**, 69–114 (2000).
27. A. Toumi, N. Piétri, T. Chiavassa, I. Couturier-Tamburelli, Acrylonitrile characterization and high energetic photochemistry at Titan temperatures. *Icarus* **270**, 435–442 (2016).
28. M. Fulchignoni, F. Ferri, F. Angrilli, A. J. Ball, A. Bar-Nun, M. A. Barucci, C. Bettanini, G. Bianchini, W. Borucki, G. Colombatti, M. Coradini, A. Coustenis, S. Debei, P. Falkner, G. Fanti, E. Flamini, V. Gaborit, R. Grard, M. Hamelin, A. M. Harri, B. Hathi, I. Jernej, M. R. Leese, A. Lehto, P. F. L. Stoppato, J. J. López-Moreno, T. Mäkinen, J. A. M. McDonnell, C. P. McKay, G. Molina-Cuberos, F. M. Neubauer, V. Pirronello, R. Rodrigo, B. Saggin, K. Schwingenschuh, A. Seiff, F. Simões, H. Svedhem, T. Tokano, M. C. Towner, R. Trautner, P. Withers, J. C. Zarnecki, In situ measurements of the physical characteristics of Titan's environment. *Nature* **438**, 785–791 (2005).
29. E. Lellouch, S. Vinatier, R. Moreno, M. Allen, S. Gulkis, P. Hartogh, J.-M. Krieg, A. Maestrini, I. Mehdi, A. Coustenis, Sounding of Titan's atmosphere at submillimeter wavelengths from an orbiting spacecraft. *Planet. Space Sci.* **58**, 1724–1739 (2010).
30. M. A. Cordiner, M. Y. Palmer, C. A. Nixon, P. G. J. Irwin, N. A. Teanby, S. B. Charnley, M. J. Mumma, Z. Kisiel, J. Serigano, Y.-J. Kuan, Y.-L. Chuang, K.-S. Wang, Ethyl cyanide on Titan: Spectroscopic detection and mapping using Alma. *Astrophys. J. Lett.* **800**, L14 (2015).
31. J. P. McMullin, B. Waters, D. Schiebel, W. Young, K. Golap, CASA architecture and applications. *Astron. Soc. Pac. Conf. Ser.* **376**, 127–130 (2007).
32. B. Bézard, R. Yelle, C. A. Nixon, *Titan: Surface, Atmosphere and Magnetosphere*, I. Mueller-Wodarg, C. Griffith, E. Lellouch, T. Cravens, Eds. (Cambridge Univ. Press, 2014), vol. 158.
33. P. G. J. Irwin, N. A. Teanby, R. de Kok, L. N. Fletcher, C. J. A. Howett, C. C. C. Tsang, C. F. Wilson, S. B. Calcutt, C. A. Nixon, P. D. Parrish, The NEMESIS planetary atmosphere radiative transfer and retrieval tool. *J. Quant. Spectrosc. Radiat. Transf.* **109**, 1136–1150 (2008).
34. J. Serigano, C. A. Nixon, M. A. Cordiner, P. G. J. Irwin, N. A. Teanby, S. B. Charnley, J. E. Lindberg, Isotopic ratios of carbon and oxygen in Titan's CO using ALMA. *Astrophys. J. Lett.* **821**, L8 (2016).
35. N. A. Teanby, P. G. J. Irwin, C. A. Nixon, R. Courtin, B. M. Swinyard, R. Moreno, E. Lellouch, M. Rengel, P. Hartogh, Constraints on Titan's middle atmosphere ammonia abundance from Herschel/SPIRE sub-millimetre spectra. *Planet. Space Sci.* **75**, 136–147 (2013).
36. H. S. P. Müller, S. Thorwirth, D. A. Roth, G. Winnewisser, The Cologne Database for Molecular Spectroscopy, CDMS. *Astron. Astrophys.* **370**, L49–L52 (2001).
37. M. A. Cordiner, C. A. Nixon, N. A. Teanby, P. G. J. Irwin, J. Serigano, S. B. Charnley, S. N. Milam, M. J. Mumma, D. C. Lis, G. Villanueva, L. Paganini, Y.-J. Kuan, A. J. Remijan, ALMA measurements of the HNC and HC3N distributions in Titan's atmosphere. *Astrophys. J. Lett.* **795**, L30 (2014).
38. C. F. Wilson, S. Guerlet, P. G. J. Irwin, C. C. C. Tsang, F. W. Taylor, R. W. Carlson, P. Drossart, G. Piccioni, Evidence for anomalous cloud particles at the poles of Venus. *J. Geophys. Res. Planets* **113**, E00B13 (2008).
39. N. A. Teanby, R. de Kok, P. G. J. Irwin, S. Osprey, S. Vinatier, P. J. Gierasch, P. L. Read, F. M. Flasar, B. J. Conrath, R. K. Achterberg, B. Bézard, C. A. Nixon, S. B. Calcutt, Titan's winter polar vortex structure revealed by chemical tracers. *J. Geophys. Res. Planets* **113**, E12003 (2008).

Acknowledgments

Funding: This research was supported by the NSF under grant no. AST-1616306, the NASA Astrobiology Institute through the Goddard Center for Astrobiology, NASA's Planetary Atmospheres and Planetary Astronomy programs, and the UK Science and Technology Facilities Council. **Author contributions:** M.Y.P. obtained and calibrated the ALMA data, performed spectral line identification, and wrote the manuscript. M.A.C. managed the project, performed the radiative transfer modeling, generated the figures, and wrote the Materials and Methods section. C.A.N. assisted in the spectral line analysis. M.A.C., C.A.N., S.B.C., and N.A.T. contributed to the structure and content of the article. Z.K. provided spectral line data and partition functions. P.G.J.I. provided and supported the NEMESIS radiative transfer code. M.J.M. provided support and supervision. **Competing interests:** The authors declare that they have no competing interests. **Data and materials availability:** This study makes use of the following ALMA data: ADS/JAO.ALMA #2012.1.00198.S, #2012.1.00261.S, #2012.1.00336.S, #2012.1.00437.S, and #2012.1.00635.S. ALMA is a partnership of ESO (representing its member states), NSF (United States), and NINS (Japan), together with NRC (Canada), MOST and ASIAA (Taiwan), and KASI (Republic of Korea), in cooperation with the Republic of Chile. The Joint ALMA Observatory is operated by ESO, AUI/NRAO, and NAOJ. The National Radio Astronomy Observatory is a facility of the NSF operated under cooperative agreement by Associated Universities Inc. The data used in this study are available from the ALMA Science Archive (https://almascience.nrao.edu/aq/). Additional data related to this paper may be requested from the authors.

Submitted 3 January 2017
Accepted 27 June 2017
Published 28 July 2017
10.1126/sciadv.1700022

Citation: M. Y. Palmer, M. A. Cordiner, C. A. Nixon, S. B. Charnley, N. A. Teanby, Z. Kisiel, P. G. J. Irwin, M. J. Mumma, ALMA detection and astrobiological potential of vinyl cyanide on Titan. *Sci. Adv.* **3**, e1700022 (2017).

ALMA detection and astrobiological potential of vinyl cyanide on Titan

Maureen Y. Palmer, Martin A. Cordiner, Conor A. Nixon, Steven B. Charnley, Nicholas A. Teanby, Zbigniew Kisiel, Patrick G. J. Irwin and Michael J. Mumma

Sci Adv **3** (7), e1700022.
DOI: 10.1126/sciadv.1700022